The Canadian Mineralogist
Vol. 44, pp. 481-495 (2006)

THE CRYSTAL STRUCTURE OF PADĚRAITE, $Cu_7(X_{0.33}Pb_{1.33}Bi_{11.33})_{\Sigma 13}S_{22}$, WITH *X* = Cu OR Ag: NEW DATA AND INTERPRETATION

DAN TOPA[§]

Department of Material Science, Division of Mineralogy, University of Salzburg, Hellbrunnerstr. 34/III, A-5020 Salzburg, Austria

EMIL MAKOVICKY

Geological Institute, University of Copenhagen, Østervoldgade 10, DK-1350 Copenhagen K, Denmark

ABSTRACT

The crystal structure of Ag-bearing paděraite, ideally $Cu_7(\mathbf{Ag_{0.33}}Pb_{1.33}Bi_{11.33})_{\Sigma 13}S_{22}$, *a* 17.585(4), *b* 3.9386(9), *c* 28.453(7) Å, β 105.41(1)°, *V* 1899.8(8) Å^3, space group $P2_1/m$ and $Z = 2$, from a skarn deposit at Băiţa Bihor in Romania, has been solved by direct methods and refined to an R_1 index of 7.72% for 2429 unique reflections [$F_o \geq 4\sigma(F_o)$] measured with Mo$K\alpha$ X-radiation on a three-circle diffractometer equipped with a CCD detector. The crystal structure of Ag-free, Cu-enriched paděraite, ideally $Cu_7(\mathbf{Cu_{0.33}}Pb_{1.33}Bi_{11.33})_{\Sigma 13}S_{22}$, *a* 17.573(2), *b* 3.9426(4), *c* 28.423(3) Å, β 105.525(2)°, *V* 1897.3(6) Å^3, space group $P2_1/m$ and $Z = 2$, from a rare-metal granitic pegmatite at Swartberg, South Africa, has been solved by direct methods and refined to an R_1 index of 5.04% for 3200 unique reflections [$F_o \geq 4\sigma(F_o)$]. In the crystal structures, there are 12 Bi sites, one Pb site, seven triangular and flat-tetrahedral Cu sites and 22 S positions. The crystal structure, in most features corresponding to that described earlier, can be represented as a intergrowth of kupčíkite-like "K slabs" and "Q slabs", which on their own make up a structure related to nordströmite or kobellite. We provide the chemical formulae and unit cells of potential KQ^n homologues of paděraite, as well as of regular intergrowths of paděraite and cuprobismutite homologous series.

Keywords: paděraite, crystal structure, single-crystal X-ray diffraction, cuprobismutite homologous series, Băiţa Bihor, Romania, Swartberg, South Africa.

SOMMAIRE

Nous avons résolu la structure cristalline de la paděraite argentifère, dont la composition idéale serait $Cu_7(\mathbf{Ag_{0.33}}Pb_{1.33}Bi_{11.33})_{\Sigma 13}S_{22}$, *a* 17.585(4), *b* 3.9386(9), *c* 28.453(7) Å, β 105.41(1)°, *V* 1899.8(8) Å^3, groupe spatial $P2_1/m$ et $Z = 2$, provenant d'un gisement de skarn à Băiţa Bihor en Roumanie, par méthodes directes, et nous l'avons affinée jusqu'à un résidu R_1 de 7.72% pour 2429 réflexions uniques [$F_o \geq 4\sigma(F_o)$] mesurées avec rayonnement Mo$K\alpha$ et un diffractomètre à trois cercles muni d'un détecteur CCD. La structure de la paděraite riche en Cu et dépourvue de Ag, dont la composition idéale serait $Cu_7(\mathbf{Cu_{0.33}}Pb_{1.33}Bi_{11.33})_{\Sigma 13}S_{22}$, *a* 17.573(2), *b* 3.9426(4), *c* 28.423(3) Å, β 105.525(2)°, *V* 1897.3(6) Å^3, groupe spatial $P2_1/m$ et $Z = 2$, provenant d'une pegmatite à éléments rares à Swartberg, en Afrique du Sud, a été résolue par méthodes directes et affinée jusqu'à un résidu R_1 de 5.04% pour 3200 réflexions uniques [$F_o \geq 4\sigma(F_o)$] mesurées avec rayonnement Mo$K\alpha$. Dans ces structures, il y a 12 sites Bi, un site Pb, sept sites Cu, soit triangulaires ou tétraédriques applatis, et 22 positions S. On peut représenter la structure, dans la plupart des aspects correspondant à celle qui est déjà connue, comme intercroissance d'un module ressemblant à la kupčíkite (plaquettes "K") et de plaquettes "Q". Ces dernières peuvent former leur propre structure, apparentée à la nordströmite ou à la kobellite. Nous présentons les formules chimiques et les mailles élémentaires des homologues KQ^n potentiels de la paděraite, de même que des intercroissances régulières de la paděraite avec la série des homologues de la cuprobismutite.

(Traduit par la Rédaction)

Mots-clés: paděraite, structure cristalline, diffraction X sur monocristaux, série des homologues de la cuprobismutite, Băiţa Bihor, Roumanie, Swartberg, Afrique du Sud.

§ *E-mail address*: dan.topa@sbg.ac.at

Introduction

Paděraite was described by Mumme & Žák (1985) as a new member of the cuprobismutite–hodrushite group with a composition $Cu_{5.9}Ag_{1.3}Pb_{1.6}Bi_{11.2}S_{22}$. It was found in the museum material from Băiţa Bihor (formerly Rezbanya), labeled as "rezbanyite", now a discredited species; this material also contained bismuthinite–pekoite intergrowths and hammarite (Mumme 1986). All the crystals used for structure investigation were found to be intergrown with these bismuthinite derivatives, so that the crystal structure of paděraite was refined to R_1 = 17% only using single-crystal diffractometer data. The *c* and *b* values of the monoclinic unit-cell (space group $P2_1/m$), 17.55 and 3.90 Å, respectively, as well as d_{010} of paděraite, as defined by Mumme (1986), are nearly identical to those of hodrushite (space group $A2/m$). Because of a substantially different β value (106.0° instead of 92.2° for hodrushite), the *a* values differ, 28.44 Å for paděraite *versus* 27.21 Å for hodrushite (Kupčík & Makovicky 1968). However, this situation simply means that $2\boldsymbol{a} + \boldsymbol{c}$ of paděraite is equal to $\boldsymbol{a}$ of hodrushite. Mumme (1986) found that the complex slabs composed of tetrahedrally coordinated copper and paired Bi pyramids are identical for both structures, but the PbS-like layer of hodrushite is replaced by a broad, split PbS-like layer with prominently inserted "aikinite-like ribbons". A three-component scheme, slicing this structure and those of the cuprobismutite–hodrushite group into *C*, *H* and *T* elements, was used to describe relations between these structures. Makovicky (1989) classified paděraite as a species *related* to (and not belonging to) the cuprobismutite homologous series. Recent chemical and HRTEM data on paděraite were published by Cook & Ciobanu (2003) and Ciobanu *et al.* (2004).

New material from Băiţa Bihor, Apuseni Mountains, Romania and Swartberg, northern Cape Province, South Africa, with chemical compositions somewhat different from the type material, and from one another, was used for new refinements of the structure. Its better quality allowed us to refine further this remarkable structure and to draw additional conclusions about the role of different elements in it. Furthermore, new understanding of this structure was achieved; it is a simple 1:1 intergrowth of a member $N = 1$ of the cuprobismutite homologous series with a layer of a novel structure-type.

Microscopic Characteristics

Paděraite invariably occurs in intimate association with the members of the cuprobismutite series and with the members of the bismuthinite–aikinite homologous series. Whereas Cook & Ciobanu (2003) and Ciobanu *et al.* (2004) described intimate intergrowths of paděraite with cuprobismutite, with some hodrushite present, in the material from Ocna de Fier, our observations suggest that the material from Băiţa Bihor and Swartberg contains parallel intergrowths or clearly defined replacement-induced aggregates in which paděraite replaces hodrushite (Fig. 1). Subhedral contacts are developed against the bismuthinite–gladite aggregates or homogeneous aikinite; these aggregates replace both paděraite and hodrushite. Emplectite forms by late replacement of both hodrushite and paděraite, as does late bismuthinite.

Chemical Composition

The composition of paděraite (Table 1) was determined by means of electron-microprobe analyses before its extraction from a polished section. A JEOL JXA–8600 electron microprobe controlled by a LINK–*eXL* system with on-line ZAF–4 correction program was used. Analytical conditions employed were 25 kV and 40 nA. The following standards (all synthetic except galena and chalcopyrite) and emission lines were selected: Bi_2S_3 (Bi$L\alpha$, S$K\alpha$), galena (Pb$L\alpha$), chalcopyrite (Cu$K\alpha$, Fe$K\alpha$), Ag metal (Ag$L\alpha$), CdTe (Cd$L\beta$, Te$L\alpha$), Sb_2S_3 (Sb$L\alpha$) and Bi_2Se_3 (Se$L\alpha$). Standard deviations (error in wt.%) of elements detected in paděraite are: Bi 0.18, Pb 0.19, S 0.06, Te and Se 0.04, Cu, Ag and Se 0.03. The chemical data for paděraite and the resulting empirical formulae are presented in Table 1. The analytical results are plotted in Figure 2, in the same way as done by Topa *et al.* (2003b) for members of the cuprobismutite homologous series. This scheme groups together the elements that occupy the same type of sites in the structure: Cu + Fe, Bi + Ag + Pb + Cd and S (Fig. 2a); the partial substitution of Bi by Cu reveals itself as deviations from the simple ratio of available cation-sites. In addition, we use a plot based on the atomic ratio of minor substituting elements (Fig. 2b), a plot in which the substituting lead was "back-calculated" to Ag and Bi (Fig. 2c), and a plot showing the Bi:Ag:Pb proportions (Fig. 2d). A relatively minor exception to the scheme used in Figure 2a arose in the case of hodrushite from Swartberg, explained in Topa *et al.* (2003b) as a result of the presence of Cu-for-Bi substitution. For the case of paděraite from the same locality, the exception is explained in the discussion of cation substitutions at the site Bi3, in this paper.

Figure 2a shows that the good resolving power of this diagram for the members of the cuprobismutite homologous series does not extend to paděraite. The latter lies close to, and partially overlaps, the field of cuprobismutite. The fields of cuprobismutite and paděraite become separated in the Fe – Ag – (Pb + Cd) and Bi – Ag – Pb plots (Figs. 2b, d), the former being a high-Ag species, whereas the latter is a high-Pb species. Both are distinguished from kupčíkite and hodrushite by the near-absence of Fe. The third plot (Fig. 2c) reflects the proportion of typical Cu(Fe) sites in each structure, resulting in better separation of paděraite from cuprobismutite than the plot in Figure 2a. However, Ag-free paděraite from Swartberg, with the Cu-for-Bi

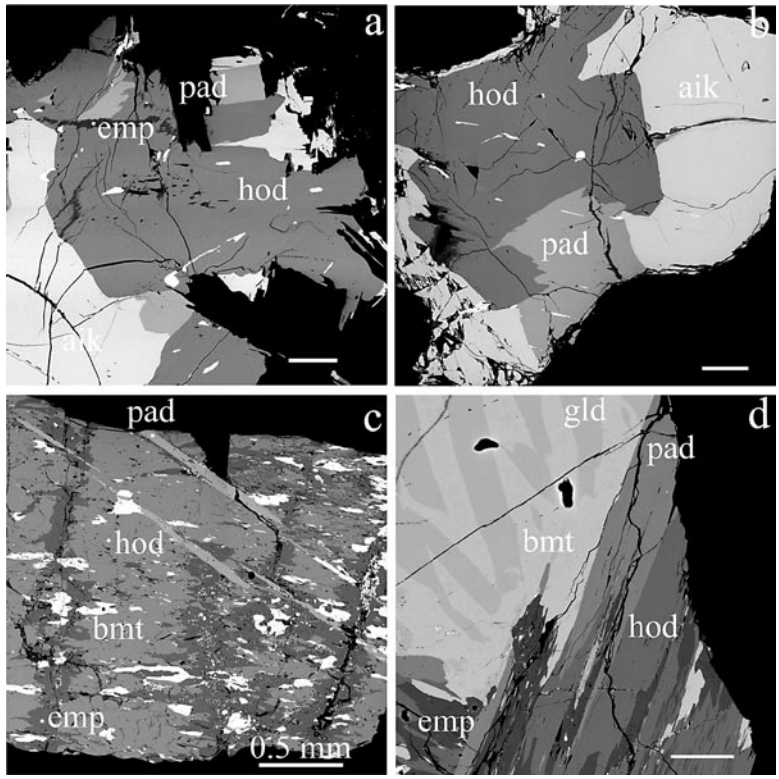

FIG. 1. Back-scattered-electron images of paděraite assemblages from: a) and b) Băiţa Bihor material, c) and d) Swartberg material. Abbreviations: pad: paděraite, hod: hodrushite, emp: emplectite, aik: aikinite, bmt: bismuthinite, gld: gladite. Where not specified, the bars represent 100 μm.

TABLE 1. AVERAGE RESULTS OF ELECTRON-PROBE ANALYSES OF PADĚRAITE

No.	sample	NA	Cu	Ag	Pb	Cd	Bi	Sb	Se	Te	S	Total	Σmet	ch	ev
1	BB-str.[1]	4	11.83(2)	0.51(1)	7.44(5)		61.88(11)	0.10(1)		0.23(1)	18.49(2)	100.48(11)	19.94	-0.14	-0.32
2	BB all	60	11.64(21)	0.76(11)	7.32(18)	0.04(8)	61.56(27)	0.04(5)	0.12(21)	0.19(4)	18.28(20)	99.95(42)	19.99	0.01	0.02
3	SB-str.[1]	6	12.08(6)		7.24(6)		61.71(24)	0.09(1)			18.33(4)	99.46(24)	20.03	0.17	0.39
4	SB all	25	12.08(9)		7.23(11)		61.96(49)	0.09(1)			18.44(12)	99.80(40)	19.99	0.06	0.15

1) $Cu_{7.09}Ag_{0.18}Pb_{1.37}(Bi_{11.28}Sb_{0.03})_{\Sigma 11.31}(S_{21.98}Te_{0.07})_{\Sigma 22.05}$ or $Cu_7\ Pb\ Bi_{11}\ (Cu_{0.09}Ag_{0.18}Bi_{0.31})_{\Sigma 0.95}\ S_{22.05}$
2) $Cu_{7.03}Ag_{0.27}(Pb_{1.36}Cd_{0.01})_{\Sigma 1.37}(Bi_{11.31}Sb_{0.01})_{\Sigma 11.32}(S_{21.89}Te_{0.07}Se_{0.06})_{\Sigma 22.01}$ or $Cu_7\ Pb\ Bi_{11}\ (Cu_{0.03}Ag_{0.27}Pb_{0.37}Bi_{0.33})_{\Sigma 0.99}\ S_{22.01}$
3) $Cu_{7.30}Pb_{1.34}(Bi_{11.35}Sb_{0.03})_{\Sigma 11.38}S_{21.97}$ or $Cu_7\ Pb\ Bi_{11}\ (Cu_{0.30}Pb_{0.34}Bi_{0.38})_{\Sigma 1.03}\ S_{21.97}$
4) $Cu_{7.28}Pb_{1.34}(Bi_{11.35}Sb_{0.03})_{\Sigma 11.38}S_{22.01}$ or $Cu_7\ Pb\ Bi_{11}\ (Cu_{0.28}Pb_{0.34}Bi_{0.38})_{\Sigma 0.99}\ S_{22.01}$

The raw data are quoted in wt.%. [1] grains used for single-crystal structural investigations. BB: sample from Băiţa Bihor, SB: sample from Swartberg; NA: number of analyses, ch: charge balance, ev: error relative to the total of valences, formulae based on 42 atoms per formula unit.

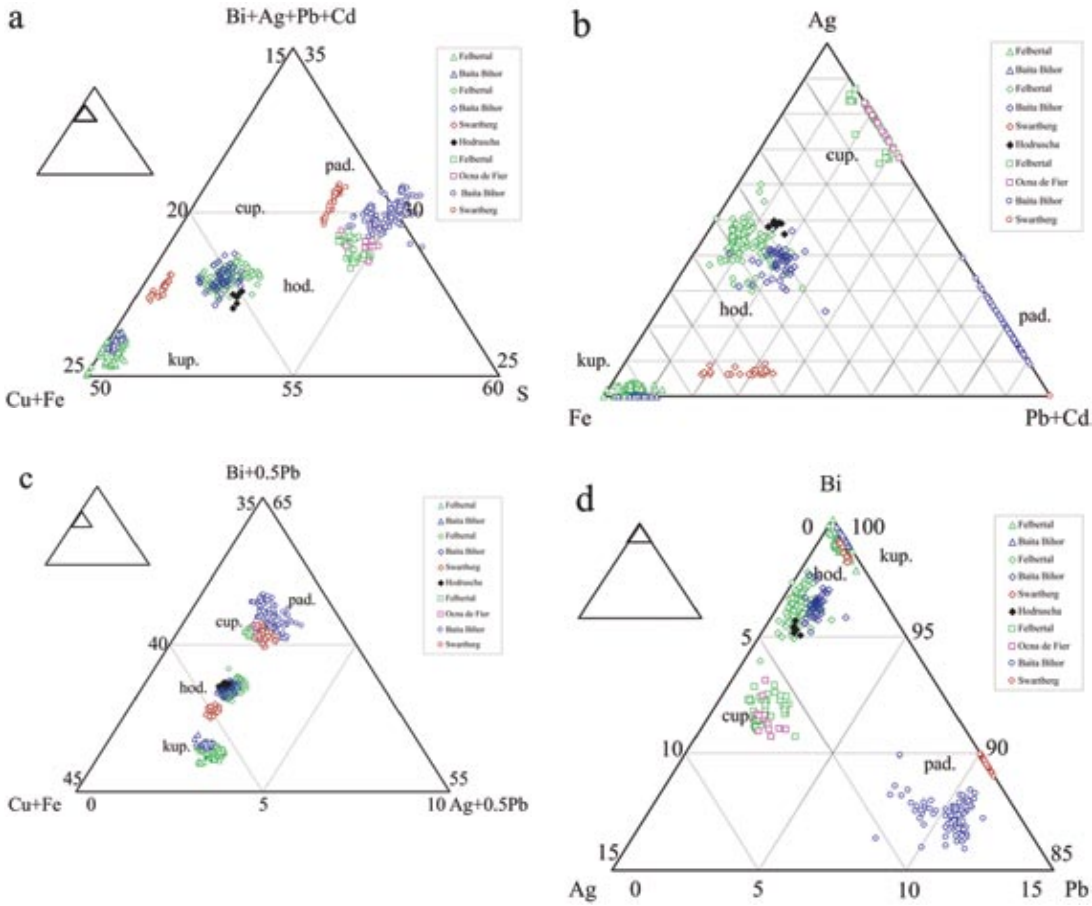

FIG. 2. Compositional diagrams for paděraite and the members of the cuprobismutite homologous series (data and provenance for the latter are listed in Topa *et al*. 2003b). An explanation of the element combinations and of the use of the diagrams for discrimination of the species involved is presented in the text.

substitution proven by the structure determination, lies separately. In this way, it is similar to Ag-free hodrushite from Swartberg (Topa *et al*. 2003b). Figures 2a through 2d indicate that a suitable combination of least two of the plots is needed for reliable discrimination of these minerals.

X-RAY DIFFRACTION AND DETERMINATION OF THE CRYSTAL STRUCTURE

Fragments of paděraite with an irregular shape and a diameter of 0.05–0.09 mm from Băiţa Bihor and Swartberg were measured on a Bruker AXS three-circle diffractometer equipped with a CCD area detector using graphite-monochromated Mo$K\alpha$ radiation. Crystal data for the fragments studied are listed in Table 2. The SMART (Bruker AXS, 1998) system of programs was used for unit-cell determination and data collection, SAINT+ (Bruker AXS, 1998) for the calculation of integrated intensities, and XPREP (Bruker AXS, 1998) for the empirical absorption-correction based on pseudo ϕ-scans. The centrosymmetric space-group $P2_1/m$, proposed by the XPREP program, was chosen, and it is consistent with the monoclinic symmetry of the lattice and intensity statistics (mean |E*E–1| = 1.119 for Băiţa Bihor and mean |E*E–1| = 1.085 for Swartberg [expected 0.968 for centrosymmetry and 0.736 for non-centrosymmetry]). The structures were solved by direct methods (program SHELXS of Sheldrick 1997a), which revealed most of the cation positions. In subsequent cycles of the refinement (program SHELXL of Sheldrick 1997b), atoms positions were deduced from difference-

Fourier syntheses by selecting from among the strongest maxima at the appropriate distances.

Experimental and refinement data are given in Table 2, fractional coordinates and isotropic displacement parameters of the atoms are listed in Table 3 and 4, and the *Me*–S bond distances for paděraite from Swartberg are presented in Table 5. Selected geometrical parameters for individual coordination-polyhedra (Balić-Žunić & Makovicky 1996, Makovicky & Balić-Žunić 1998), calculated with the IVTON program (Balić-Žunić & Vicković 1996), are given in Table 6. The structure of paděraite (for both occurrences) is presented in Figure 3, and the site labeling, in Figure 4. The tables of structure factors, anisotropic displacement parameters, as well as of bond distances and geometrical parameters of polyhedra in paděraite from Băiţa Bihor may be obtained from the Depository of Unpublished Data, CISTI, National Research Council, Ottawa, Ontario K1A 0S2, Canada.

TABLE 2. SINGLE-CRYSTAL X-RAY DIFFRACTION: EXPERIMENTAL AND REFINEMENT DETAILS

Crystal data	Ag-bearing paděraite Băiţa Bihor, Romania	Cu-enriched paděraite Swartberg, South Africa
Chemical formula	Cu_7 $(Cu_{0.09}\mathbf{Ag_{0.18}}$ $Pb_{1.37}Bi_{11.31})_{\Sigma 12.86}S_{22.05}$	Cu_7 $(\mathbf{Cu_{0.30}}Pb_{1.34}$ $Bi_{11.38})_{\Sigma 13.03}S_{21.97}$
Chemical formula weight	7658.01	7644.93
Cell setting	Monoclinic	Monoclinic
Space group	$P2_1/m$	$P2_1/m$
a (Å)	17.585(4)	17.573(2)
b (Å)	3.9386(9)	3.9426(4)
c (Å)	28.453(7)	28.423(3)
β (°)	105.41(1)	105.525(2)
V (Å^3)	1899.8(8)	1897.3(6)
Z	2	2
D_x (g/cm^3)	6.694	6.691
No. of reflections for cell-parameters	1656	3119
μ (mm^{-1})	63.325	63.66
Shape of crystal	irregular	irregular
Size of crystal (mm)	0.03 x 0.03 x 0.04	0.03 x 0.035 x 0.07
Color of crystal	black	black
Data collection		
T_{min}	0.1895	0.0506
T_{max}	0.6621	0.2881
No. of measured reflections	16039	28416
No. of independent reflections	5327	5266
No. of observed reflections	2429	3200
Criterion for observed reflections	$I > 2\sigma(I)$	
R_{int}	25.34%	24.48%
θ_{max} (°)	28.38	28.29
Range of h, k, l	$-17 < h < 23$	$-23 < h < 22$
	$-5 < k < 5$	$-5 < k < 5$
	$-37 < l < 38$	$-37 < l < 37$
Refinement		
Refinement on F_o^2		
$R_1[F_o^2>2\sigma(F_o^2)]$	7.72%	5.04%
$wR(F_o^2)$	23.17%	13.61%
S (*GooF*)	0.886	0.707
No. of reflections used in refin.	2429	3200
No. of parameters refined	250	252
Weighting scheme	$w = 1/[\sigma^2(F_o^2) + (0.0825P)^2]$	$w = 1/[\sigma^2(F_o^2) + (0.0782P)^2]$
	where $P = (F_o^2 + 2F_c^2)/3$	
$(\Delta/\sigma)_{max}$	0.01	0.01
$\Delta\rho_{max}$ (e/Å^3)	5.70	4.83
$\Delta\rho_{min}$ (e/Å^3)	-9.98	-3.27
Extinction method	none	
Source of atomic scattering factors	International Tables for X-Ray Crystallography (1992, Vol. C, Tables 4.2.6.8 and 6.1.1.4)	
Computer programs		
Structure solution	*SHELXS97* (Sheldrick 1997a)	
Structure refinement	*SHELXL97* (Sheldrick 1997b)	

DESCRIPTION OF THE STRUCTURE

Coordination polyhedra

The crystal structure of paděraite contains 13 large-cation polyhedra, seven triangular and flattened tetrahedral Cu sites, and 22 sulfur sites. All of them lie on reflection planes of the space group, but have general x and z coordinates.

TABLE 3. SITE LABELS, OCCUPANCY FACTORS, FRACTIONAL COORDINATES AND EQUIVALENT ISOTROPIC-DISPLACEMENT PARAMETERS OF ATOMS IN PADĚRAITE FROM BĂIŢA BIHOR

ATOM[a]	*x/a*	*y/b*	*z/c*	sof	U_{iso}
Pb (*Me*2)	0.34195(13)	0.25	0.18032(8)		0.0298(6)
Bi1 (*Me*5)	0.27360(11)	0.75	0.62006(7)		0.0144(4)
Bi2 (*Me*6)	0.29355(10)	0.75	0.77468(7)		0.0136(4)
Bi3[b] (*Me*7)	0.28837(17)	0.75	0.92156(10)	0.710(5)	0.0222(10)
Ag3[b] (*Me*7)	0.2343(8)	0.75	0.9400(5)	0.290(5)	0.0222(10)
Bi4 (*Me*10)	0.22884(11)	0.75	0.38139(7)		0.0145(4)
Bi5 (*Me*13)	0.11975(11)	0.25	0.82186(7)		0.0145(4)
Bi6 (*Me*14)	0.10532(11)	0.75	0.00502(7)		0.0179(5)
Bi7 (*Me*15)	0.09598(13)	0.25	0.13563(7)		0.0220(5)
Bi8 (*Me*16)	0.05401(10)	0.25	0.28225(7)		0.0133(4)
Bi9 (*Me*17)	0.01535(10)	0.75	0.57041(7)		0.0130(4)
Bi10 (*Me*18)	0.48282(11)	0.75	0.42972(7)		0.0134(4)
Bi11 (*Me*19)	0.45935(10)	0.25	0.71944(7)		0.0126(4)
Bi12 (*Me*20)	0.48094(11)	0.25	0.87687(7)		0.0154(4)
Cu1 (*Me*3)	0.3705(5)	0.25	0.3059(3)		0.033(2)
Cu2 (*Me*4)	0.3394(4)	0.25	0.4914(3)		0.023(2)
Cu3 (*Me*8)	0.3117(4)	0.25	0.0656(3)		0.022(2)
Cu4 (*Me*9)	0.2284(5)	0.75	0.2548(3)		0.036(2)
Cu5 (*Me*11)	0.1616(4)	0.25	0.5103(3)		0.025(2)
Cu6 (*Me*12)	0.1320(5)	0.25	0.6962(2)		0.031(2)
Cu7 (*Me*1)	0.5838(7)	0.75	0.9978(4)		0.102(5)
S1	0.4308(6)	0.75	0.6491(4)		0.010(2)
S2	0.4743(7)	0.75	0.7974(5)		0.012(2)
S3	0.4725(8)	0.75	0.9449(6)		0.022(3)
S4	0.3659(7)	0.75	0.1041(5)		0.019(3)
S5	0.3795(7)	0.75	0.2662(5)		0.020(3)
S6	0.3845(7)	0.25	0.3866(4)		0.090(2)
S7	0.4126(7)	0.75	0.4988(4)		0.014(3)
S8	0.2891(7)	0.25	0.5616(5)		0.016(3)
S9	0.2919(6)	0.25	0.7047(4)		0.008(2)
S10	0.2987(8)	0.25	0.8450(5)		0.018(3)
S11	0.2854(9)	0.25	0.9815(6)		0.036(4)
S12	0.2049(7)	0.75	0.1716(5)		0.013(3)
S13	0.2050(7)	0.25	0.2922(4)		0.010(2)
S14	0.2123(7)	0.25	0.4392(4)		0.013(3)
S15	0.1133(7)	0.25	0.6146(4)		0.013(3)
S16	0.1335(7)	0.75	0.7416(5)		0.015(3)
S17	0.1233(7)	0.75	0.8872(4)		0.013(3)
S18	0.0066(7)	0.75	0.0553(4)		0.013(3)
S19	0.0335(7)	0.75	0.2050(5)		0.017(3)
S20	0.0746(6)	0.75	0.3533(4)		0.010(2)
S21	0.0888(7)	0.75	0.5022(5)		0.015(3)
S22	0.1776(7)	0.25	0.0665(5)		0.017(3)

sof: site-occupancy factor. a: The site labels follow the structure refinements of paděraite by Mumme (1986). b: New split position (this study).

The only internal Bi site in the block of the PbS archetype is Bi2, the rest being on the surface of the block. From these, Bi1 Bi3 and Bi4 are most exposed. Atoms Bi9 and Bi10 form columns of paired Bi coordination pyramids at $z = 1/2$, whereas Bi6 (central) and Bi7 (apical) form four-fold ribbons of Bi pyramids at $z = 0$ (Fig. 4). These were interpreted in the literature (Mumme 1986) as bismuthinite-like ribbons, but the complete coordination-polyhedra of Bi6 and Bi7 are just the opposite of the coordinations observed at each respective site in bismuthinite.

In their complete monocapped trigonal coordination prisms, Bi1, Bi4, Bi6, Bi9 and Bi10 exhibit the most pronounced lone-electron-pair activity, as confirmed by the highest eccentricity in their coordination polyhedra (Table 6). The minimum eccentricity is observed for the sites Bi2 and Bi11, surrounded by other polyhedra of the PbS-like portion of the structure. The spread of the Bi–S distances (Table 5) follows the same trend. The sites Bi2 and Bi7 show anomalously long values (2.72 Å) for the shortest *Me*–S distances in both structures, if compared to Bi1 or Bi4. Therefore, they apparently host the excess Pb shown by chemical analyses (Table 1), but not accounted for by the typical single Pb site with low eccentricity, situated at one corner of the PbS-like block.

Bi3 is a partially occupied octahedral site (~70% occupancy), combined with a ~30% occupied trigonal planar Cu (in the Băiţa Bihor material) or Ag site (in the Swartberg material). The problematically long Bi3–S17 bond (>2.8 Å) should be the shortest bond of the Bi3 coordination polyhedron, expected to be about 2.6 Å. In parallel, the Cu(Ag)–S17 bond is unacceptably short by about 0.2 Å. Therefore, we deem the S17 position to be an average of S positions from the mixture of about 30% of a Cu(Ag) polyhedron and 70% of a Bi polyhedron in the "Bi3" string of polyhedra along [010].

The arrays of copper sites can be divided into three categories:

1) the trigonal planar Cu(Ag) in a trigonal planar "*X*" site in a triangular wall of an unoccupied Bi3 octahedron, as already discussed. Although it has been successfully refined as Ag for the Băiţa Bihor material, giving a very reasonable value of the occupancy, the *Me*–S distances are compatible with those of Cu as well, if, in the light of the statistical nature of the S positions described above, they can be used at all. The *X* site is the only Ag-containing site found in the current structural determination; in the Ag-free Swartberg material, it is the site of a Cu-for-Bi substitution.

2) distorted tetrahedral sites Cu1 to Cu6, transitional to the trigonal planar coordination, especially in the case of Cu1 and Cu2. All of them can be completed to trigonal bipyramidal coordinations with varying degree of deviation from the central trigonal planes of the three coordination bipyramids. The pair Cu1–Cu4 has an analogy in kupčíkite (Topa *et al.* 2003a) as sites Cu(Fe)2–Cu3, whereas Cu6 is located in a manner analogous to Cu1 in cuprobismutite (Topa *et al.* 2003b).

3) a distorted linear coordination Cu7 with two additional longer and two very long distances to four additional S atoms, forming a very flattened coordination octahedron [2 + 4]. This is the site in which Mumme (1986) placed Ag, with the Ag–S distances 2.16 and 2.37 Å. Our occupancy and *Me*–S distances of 2.13–2.22 Å suggest a pure copper site.

The [010] string of trigonal coordination bipyramids of Cu1 and Cu4 leads to a string of Cu–Cu distances equal to 3.2 Å, parallel to [010]. The edge-sharing tetrahedron Cu2 and Cu5 and the edge-sharing, very distorted tetrahedron Cu7–Cu7 generate Cu–Cu distances of 3.32 Å and 3.37 Å, respectively, along [100]. The Cu3–Cu7 distance is 2.97 Å, whereas Cu6 and Cu*X* appear to have no cation neighbors. This

TABLE 4. SITE LABELS, OCCUPANCY FACTORS, FRACTIONAL COORDINATES AND EQUIVALENT ISOTROPIC-DISPLACEMENT PARAMETERS OF ATOMS IN PADĚRAITE FROM SWARTBERG

ATOM [a]	*x/a*	*y/b*	*z/c*	sof	U_{iso}
Pb	0.34249(7)	0.25	0.18024(5)		0.0289(3)
Bi1	0.27356(6)	0.75	0.62010(4)		0.0143(2)
Bi2	0.29351(6)	0.75	0.77480(4)		0.0126(2)
Bi3 [b]	0.28975(9)	0.75	0.92193(6)	0.680(2)	0.0177(5)
Cu8 [b]	0.23585(72)	0.75	0.93998(49)	0.320(2)	0.024(4)
Bi4	0.22882(6)	0.75	0.38128(4)		0.0144(2)
Bi5	0.12012(6)	0.25	0.82221(4)		0.0134(2)
Bi6	0.10540(6)	0.75	0.00493(4)		0.0157(2)
Bi7	0.09656(7)	0.25	0.13544(4)		0.0205(3)
Bi8	0.05403(6)	0.25	0.28183(4)		0.0131(2)
Bi9	0.01533(6)	0.75	0.57052(4)		0.0135(2)
Bi10	0.48293(6)	0.75	0.42963(4)		0.0130(2)
Bi11	0.45939(6)	0.25	0.71975(4)		0.0127(2)
Bi12	0.48079(6)	0.25	0.87746(4)		0.0135(2)
Cu1	0.3708(3)	0.25	0.3058(1)		0.0313(9)
Cu2	0.3396(2)	0.25	0.4906(1)		0.0225(8)
Cu3	0.3119(2)	0.25	0.0652(1)		0.0244(9)
Cu4	0.2286(3)	0.75	0.2544(2)		0.0308(9)
Cu5	0.1616(2)	0.25	0.5104(2)		0.0235(8)
Cu6	0.1335(3)	0.25	0.6968(1)		0.0314(9)
Cu7	0.4187(4)	0.25	0.0002(3)		0.120(3)
S1	0.4313(4)	0.75	0.6494(3)		0.012(1)
S2	0.4753(4)	0.75	0.7988(3)		0.016(1)
S3	0.4711(4)	0.75	0.9446(3)		0.015(1)
S4	0.3662(4)	0.75	0.1037(3)		0.013(1)
S5	0.3797(4)	0.75	0.2655(3)		0.012(1)
S6	0.3839(4)	0.25	0.3869(3)		0.013(1)
S7	0.4119(4)	0.75	0.4986(3)		0.012(1)
S8	0.2887(4)	0.25	0.5614(3)		0.013(1)
S9	0.2929(4)	0.25	0.7044(3)		0.011(1)
S10	0.2987(4)	0.25	0.8452(3)		0.010(1)
S11	0.2891(5)	0.25	0.9816(3)		0.025(2)
S12	0.2053(4)	0.75	0.1715(3)		0.013(1)
S13	0.2046(4)	0.25	0.2928(3)		0.014(1)
S14	0.2126(4)	0.25	0.4398(3)		0.012(1)
S15	0.1126(4)	0.25	0.6148(3)		0.014(1)
S16	0.1328(4)	0.75	0.7415(3)		0.013(1)
S17	0.1245(4)	0.75	0.8876(3)		0.017(2)
S18	0.0048(4)	0.75	0.0558(3)		0.014(1)
S19	0.0337(4)	0.75	0.2047(3)		0.014(1)
S20	0.0739(4)	0.75	0.3522(3)		0.013(1)
S21	0.0894(4)	0.75	0.5033(3)		0.010(1)
S22	0.1788(4)	0.25	0.0663(3)		0.013(1)

sof: site-occupancy factor. a: The site labels follow those used in the structure refinements of paděraite by Mumme (1986). b: New split position (this study).

TABLE 5. SELECTED INTERATOMIC Bi–S, Pb–S, Ag–S AND Cu–S DISTANCES (Å) FOR PADĚRAITE FROM SWARTBERG

Pb		Bi1		Bi2		Bi3		Cu8		Bi4		Bi5	
S4	3.047(7)	S8	2.642(6)	S16	2.728(7)	S11	2.602(6)	S17	2.118(13)	S20	2.625(7)	S19	2.605(7)
S4	3.047(7)	S8	2.642(6)	S10	2.793(4)	S11	2.602(6)	S11	2.360(8)	S14	2.643(4)	S17	2.696(6)
S5	3.056(6)	S1	2.672(7)	S10	2.793(4)	S17	2.805(7)	S11	2.360(8)	S14	2.643(4)	S17	2.696(6)
S5	3.056(6)	S9	3.051(7)	S9	2.807(6)	S10	2.975(5)			S13	3.133(7)	S10	3.029(5)
S12	3.072 6)	S9	3.051(7)	S9	2.807(6)	S10	2.975(5)			S13	3.133(7)	S16	3.080(5)
S12	3.072(6)	S15	3.418(6)	S2	3.079(7)	S3	3.078(7)			S6	3.331(6)	S16	3.080(5)
S2	3.100(7)	S15	3.418(6)							S6	3.331(6)		
Bi6		**Bi7**		**Bi8**		**Bi9**		**Bi10**		**Bi11**		**Bi12**	
S18	2.566(9)	S22	2.736(7)	S13	2.580(7)	S21	2.583(7)	S7	2.583(9)	S5	2.745(7)	S4	2.596(7)
S22	2.717(4)	S12	2.746(5)	S20	2.763(4)	S15	2.691(4)	S6	2.695(4)	S1	2.757(6)	S3	2.780(6)
S22	2.717(4)	S12	2.746(5)	S20	2.763(4)	S15	2.691(4)	S6	2.695(4)	S1	2.757(6)	S3	2.780(6)
S18	2.971(5)	S18	3.107(6)	S19	2.898(6)	S21	3.099(4)	S7	3.078(5)	S9	2.840(7)	S2	2.962(7)
S18	2.971(5)	S18	3.107(6)	S19	2.898(6)	S21	3.099(4)	S7	3.078(5)	S2	2.946(6)	S2	2.962(7)
S17	3.440(9)	S19	3.185(7)	S16	3.171(7)	S20	3.607(6)	S1	3.608(8)	S2	2.946(6)	S10	3.084(5)
		S19	3.185(7)			S20	3.607(6)	S1	3.608(8)				
Cu1		**Cu2**		**Cu3**		**Cu4**		**Cu5**		**Cu6**		**Cu7**	
S6	2.256(9)	S14	2.311(7)	S11	2.303(9)	S12	2.282(9)	S8	2.314(7)	S15	2.259(9)	S3	2.143(9)
S5	2.305(5)	S7	2.324(4)	S4	2.331(4)	S13	2.345(6)	S21	2.325(4)	S16	2.346(4)	S11	2.196(11)
S5	2.305(5)	S7	2.324(4)	S4	2.331(4)	S13	2.345(6)	S21	2.325(4)	S16	2.346(4)	S3	2.828(9)
S13	2.844(9)	S8	2.410(9)	S22	2.346(8)	S5	2.589(9)	S14	2.407(8)	S9	2.751(9)	S3	2.828(9)

TABLE 6. CHARACTERISTICS OF THE POLYHEDRA IN THE REFINED STRUCTURE OF PADĚRAITE FROM SWARTBERG

	Sphere radius (Å)	Volume distorsion	Volume-based eccentricity	Volume-based sphericity	Sphere volume (Å^3)	Polyhedron volume (Å^3)
Pb	3.064	0.1011	0.0095	0.9823	120.471	40.978
Bi1	2.979	0.1230	0.4444	0.9175	110.781	36.766
Bi2	2.836	0.0049	0.1788	0.9456	95.572	30.271
Bi3	2.833	0.0027	0.2784	0.9168	95.274	30.246
Cu8	2.262	0.0000	0.3550	1.0000	48.486	0.000
Bi4	2.972	0.1173	0.4409	0.9716	109.954	36.728
Bi5	2.859	0.0056	0.3079	0.9669	97.930	30.997
Bi6	2.938	0.1494	0.4062	0.9597	106.252	28.767
Bi7	3.004	0.1494	0.3395	0.9900	113.600	36.564
Bi8	2.855	0.0139	0.2893	0.9853	97.502	30.605
Bi9	3.079	0.1419	0.5387	0.9254	122.295	39.713
Bi10	3.076	0.1429	0.5348	0.9234	121.866	39.526
Bi11	2.831	0.0045	0.1452	0.9717	95.000	30.102
Bi12	2.858	0.0039	0.2647	0.9823	97.833	31.020
Cu1	2.374	0.0160	0.4929	1.0000	56.053	6.757
Cu2	2.334	0.0408	0.0982	0.9999	53.232	6.256
Cu3	2.327	0.0220	0.0376	1.0000	52.778	6.324
Cu4	2.373	0.0218	0.2637	1.0000	55.992	6.710
Cu5	2.335	0.0401	0.0931	0.9999	53.307	6.269
Cu6	2.371	0.0282	0.4199	0.9999	55.818	6.646
Cu7	2.426	0.0375	0.6050	1.0000	59.809	7.053

In addition to the original sources (Balić-Žunić & Makovicky 1996, Makovicky & Balić-Žunić 1998), consult also the appendix in Topa *et al.* (2003b) for the definition and meaning of these parameters.

survey shows that only the Cu3–Cu7 distance suggests a weak cation–cation interaction.

Our structure determinations show that the chemical differences between the two samples of paděraite have only a minor influence on the structure configurations. The principal difference, the presence or absence of Ag, concentrates in a single structural site, Bi3/*X*. A limited variation in the chemical composition of the mineral can be expected, in which the increase in the (Cu + Ag) substitution in the Bi3 site is correlated with the reduction of the Pb contents in the mixed (Bi, Pb) sites. This leads to a formula $Cu_7Pb[(Cu,Ag)_xBi_{1-x}(Bi_{2-y}Pb_y)]Bi_9S_{22}$, where $y = 1 - 2x$. Preserving the same scheme of cation sites, hypothetical extreme compositions for paděraite are $Cu_7Pb[Bi(BiPb)]Bi_9S_{22}$ and $Cu_7Pb[(Cu,Ag)_{0.5}Bi_{0.5}(Bi_2)]Bi_9S_{22}$. The observed chemical and structural composition for paděraite from both localities has $x = y \approx 0.33$ (Tables 1, 3, 4).

Modular description

Our studies confirm the structure derived by Mumme (1986) in all important features and site assignments. The only substantial difference is that in our refinements, the Cu7 site results in a clear Cu position, whereas Mumme (1986) assigned this position to Ag.

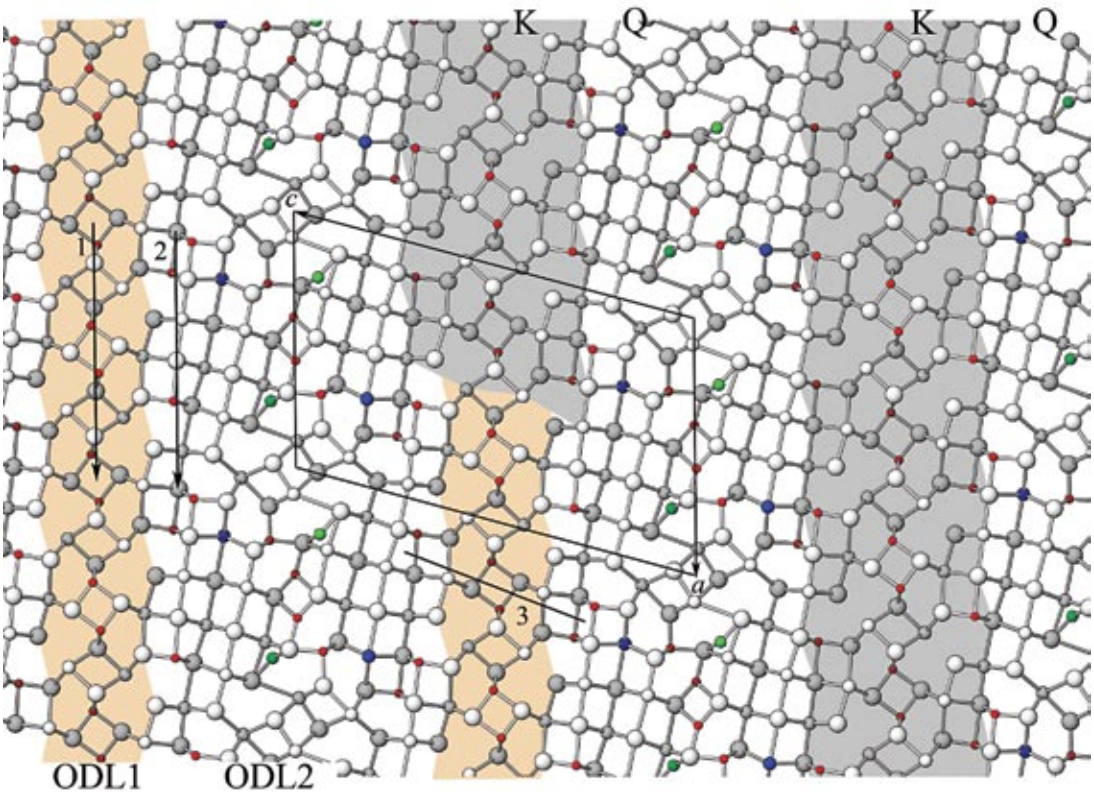

FIG. 3. The crystal structure of paděraite in projection on (010), with atoms at $y = 0.25$ (white) and at 0.75 (grey shading), respectively. In the order of decreasing size, the circles represent S, Pb (blue), *X* position (Cu or Ag, green), Bi, and Cu (red). The right-hand side of the figure shows Q modules (unshaded) between slabs (001) of kupčikite-like structure denoted as K modules (shaded in grey). Orange and intervening uncolored slabs in the left-hand side of the figure are the OD layers of Type 1 and Type 2, respectively. Arrows 1 and 2 show vectors (***a*** + ***b***) discussed in the text, whereas line segment 3 interconnects configurations of Cu polyhedra used to illustrate the potential OD phenomena in paděraite.

The Bi3 site combines with the "*X* site" into a column of octahedra with a mixed cation-occupancy; this was beyond the quality limitations of Mumme's material.

The crystal structure of paděraite can be understood in a number of ways. Mumme (1986) defined "*C* layers" comprising a repeat period *d*(001) of $Cu_4Bi_5S_{10}$ (Mariolacos *et al*. 1975) *minus* the Bi octahedron at 0, 0, 0, and "*D* layers", which are the excess zig-zag layers (100) in cuprobismutite once the *C* layers have been subtracted. Then Mumme approximated paděraite as a $^1C^4D$ polysome, whereas $Cu_4Bi_5S_{10}$ is $^1C^0D$, cuprobismutite $^1C^1D$, and hodrushite $^2C^1D$, not involving the complex centers of ^4D layers in paděraite and the "leftover" octahedra in $Cu_4Bi_5S_{10}$. For details of this scheme, the reader is referred to the original paper by Mumme (1986).

The new interpretation, presented here (Fig. 3), describes paděraite as a regular 1:1 intergrowth of K and Q modules. The K modules are complete kupčíkite slabs, *i.e*., ($Cu_4Bi_5S_{10}$)-like, with boundaries drawn through the central regular Bi octahedra of the kupčíkite structure (Topa *et al*. 2003a) and between planar copper sites. Thus their thickness is the d_{100} value of kupčíkite, and they are not identical with the "kupčíkite-like layers" used in the definition of the cuprobismutite homologues (Topa *et al*. 2003a, b).

The Q modules (Fig. 3) are a type of slab with a close structural and configurational affinity to nordströmite (Mumme 1980).

If the Q slabs are removed, the kupčíkite-like K slabs collapse directly into a complete, undistorted structure of kupčíkite (not presented here; see Topa *et al*. 2003a, b). The alternating Q slabs can be joined either by a direct collapse along [101] of paděraite, yielding a QQ structure of a sheared layer type (Fig. 5) similar to nordströmite, or with a shift of ½ (***a*** + ***b***), resulting in another structure (QQ'), composed of rods

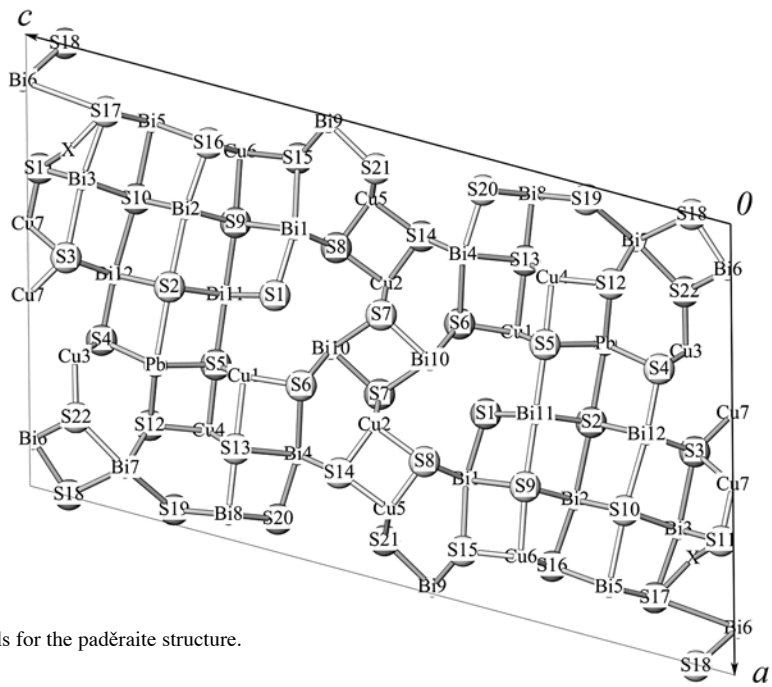

FIG. 4. Site labels for the paděraite structure.

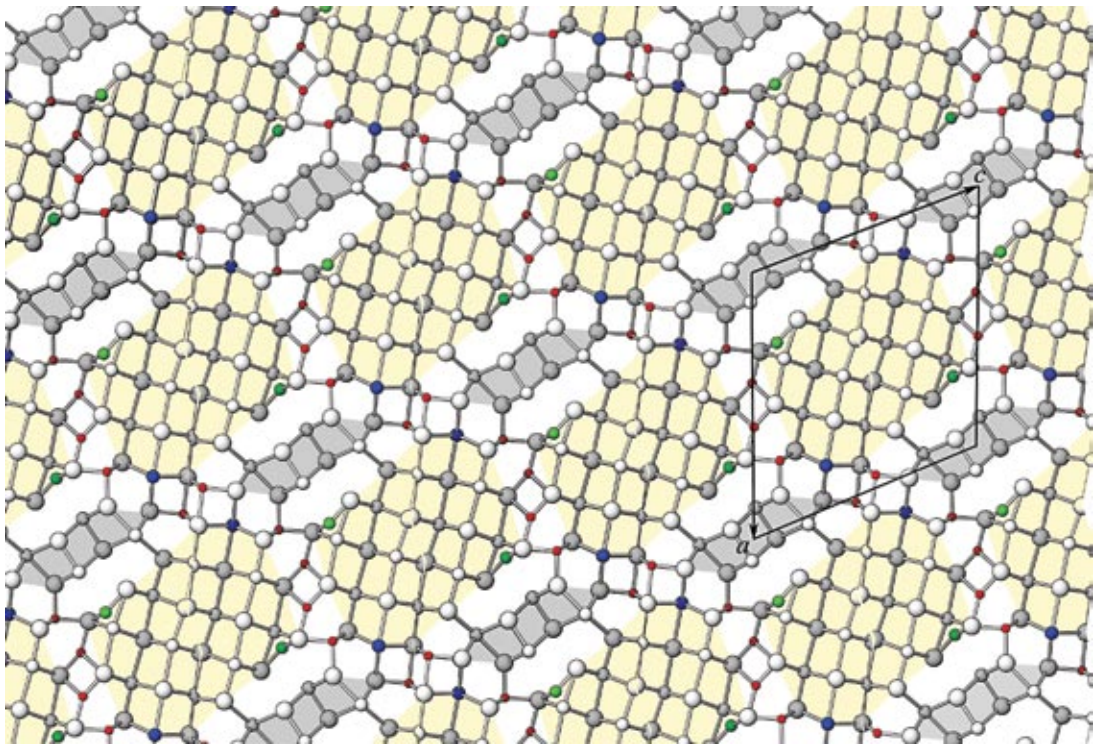

FIG. 5. A hypothetical Cu–Pb(Ag)–Bi sulfosalt composed of a pure QQ module sequence. Sheared levels of triple octahedra are yellow, "Bi_4S_6" elements are grey. Figures 5–6 and 8–10 are collages combining segments of known structures.

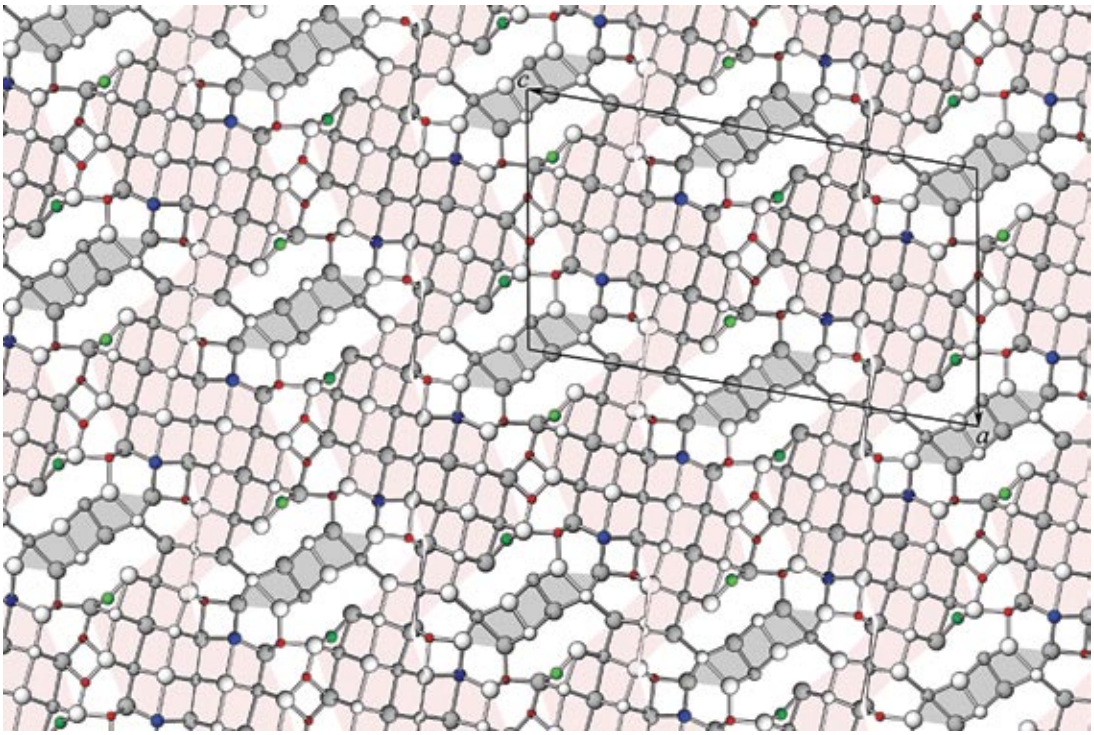

FIG. 6. A hypothetical derivative of paděraite with a QQ' sequence of Q modules. Configurations based on the PbS-archetype are outlined in pink.

of PbS-like arrangement interconnected by layers of octahedra (Fig. 6).

The structure of nordströmite, $CuPb_3Bi_7(S,Se)_{14}$, (Mumme 1980) (Fig. 7), considered in connection with the Q modules, is composed of double layers of octahedra that are periodically sheared every 2½ pseudohexagonal subperiods, altering the octahedra involved into split octahedra (CN = 7). These layers are interleaved by fragments of pseudotetragonal layers, four tetragonal subcells long. Adjacent fragments are offset *en échelon* by the same shear planes as the layers of octahedra. The *loci* of the offsets are occupied by a pair of trigonal planar Cu atoms; their full coordination-polyhedra are trigonal bipyramids. In the hypothetical layered QQ structure derived from paděraite (Fig. 5), the pseudotetragonal fragments are two subcells (*i.e.*, coordination pyramids) wide, and the paired trigonal bipyramids of Cu in shear planes correspond to those in nordströmite. The pseudohexagonal layers (marked in yellow in Fig. 5) are three layers of octahedra thick, and the sheared portions differ from those in nordströmite. In the QQ structure, they are filled by linearly coordinated Cu, the coordination of which is completed to extremely broad and somewhat asymmetrically occupied octahedra (CN = 2 + 4). If we compare the scheme of Bi, Pb octahedra in the adjacent yellow fragments, we can describe their displacement as a shear of layers of octahedra by ½ d_{100} of the PbS-like array. This Cu-rich, sheared interval is capped on both sides by Cu tetrahedra, absent in nordströmite.

In the other, QQ' structural alternative (Fig. 6), the rods of PbS archetype remind one of those in kobellite (Miehe 1971). They are, however, reduced in width, and have a parallel orientation. They are interconnected by short $(111)_{PbS}$ intervals; the intervening space hosts the Bi_4S_6 ribbons, and the rod–rod contacts are filled with Cu polyhedra. This structural arrangement reminds one of the "boxwork" structure-type of complex sulfosalts (*e.g.*, the structure of neyite, Makovicky *et al.* 2001).

The structural formula of the hypothetical QQ phase, or of its QQ' variant, is $^{[4]}Cu\ ^{[3]}Cu\ ^{[2]}Cu\ ^{[7]}M\ ^{[8]}M_2\ ^{[6]}M_5\ S_{12}$, where "Cu" = Cu, Ag, and M = Bi, Pb. This results in the possible formula $Cu_{3-x}Ag_xPb_3Bi_5S_{12}$; in paděraite, less Pb is present in this layer because the kupčíkite portion requires additional positive charges (Topa *et al.* 2003a, b), which causes a part of the Pb to be replaced by Bi.

POLYTYPISM

In the crystal structure of paděraite, the (001) slabs, composed of Bi_2S_4 columns and of the paired CuS_4 tetrahedra, have a (100) periodicity equal to a half of the ($\boldsymbol{a}$ + $\boldsymbol{b}$) period valid for the bulk of the structure (Fig. 3). This can be seen if one follows the pair of nearly identical Cu2 and Cu5 tetrahedra along the ($\boldsymbol{a}$ + $\boldsymbol{b}$) direction (arrow 1 in Fig. 3) and notes the nature of adjacent structural configurations (*e.g.,* along arrow 2 in Fig. 3). This 1:2 mismatch leads to a potential polytypism in paděraite.

For a description of this phenomenon, two distinct OD layers have to be selected (Fig. 3). The first OD layer (ODL1, Fig. 3) includes the Bi9 and Bi10 columns and the paired Cu2 and Cu5 tetrahedra; the boundary with the second OD layer (ODL2, Fig. 3) runs through Bi1 and Bi4, as well as S1 and S20 (Fig. 4), which also obey the halved periodicities of the *C*-centered ODL1 layer. In the ODL2 layer, however, Bi1 forms part of a "cuprobismutite-like" arrangement around Cu6, whereas Bi4 forms part of a "kupčíkite-like" arrangement of Cu1 and Cu4 (Figs. 3, 4); therefore, these two cation sites are crystallographically non-equivalent.

In the paděraite structure growing along the d_{001} direction, an ODL2 layer can attach itself to the ODL1 layer in two positions, ($\boldsymbol{a} + \boldsymbol{b}$)/2 of paděraite apart. They can be recognized by inspecting the above-mentioned copper configurations Cu1, Cu4 and Cu6, which face one another across ODL1, when passing through the Cu2–Cu5 configuration. Different configurations face one another in the known polytype of paděraite (line segment 3 in Fig. 3), whereas the identical configurations face one another in the hypothetical polytype (line segments 1 and 2 in Fig. 8). The latter configuration might be marginally less stable than the former one, and has not been observed in nature to date. The resulting unit-cells are presented in Table 7. The symmetry of the OD layers is $C2/m$ for ODL1, and $P2_1/m$ for ODL2. In projection onto the OD layers, the origins of the two layers are shifted by $^1/_8$ a for paděraite and $\sim^1/_4$ a for the hypothetical polytype. The resulting unit-cells are $P2_1/m$ and $A2/m$, the latter with doubled d_{001} (entries 1 and 8 in Table 7).

STRUCTURAL SERIES

The structural compatibility of paděraite and cuprobismutite homologues, noticed already by Mumme

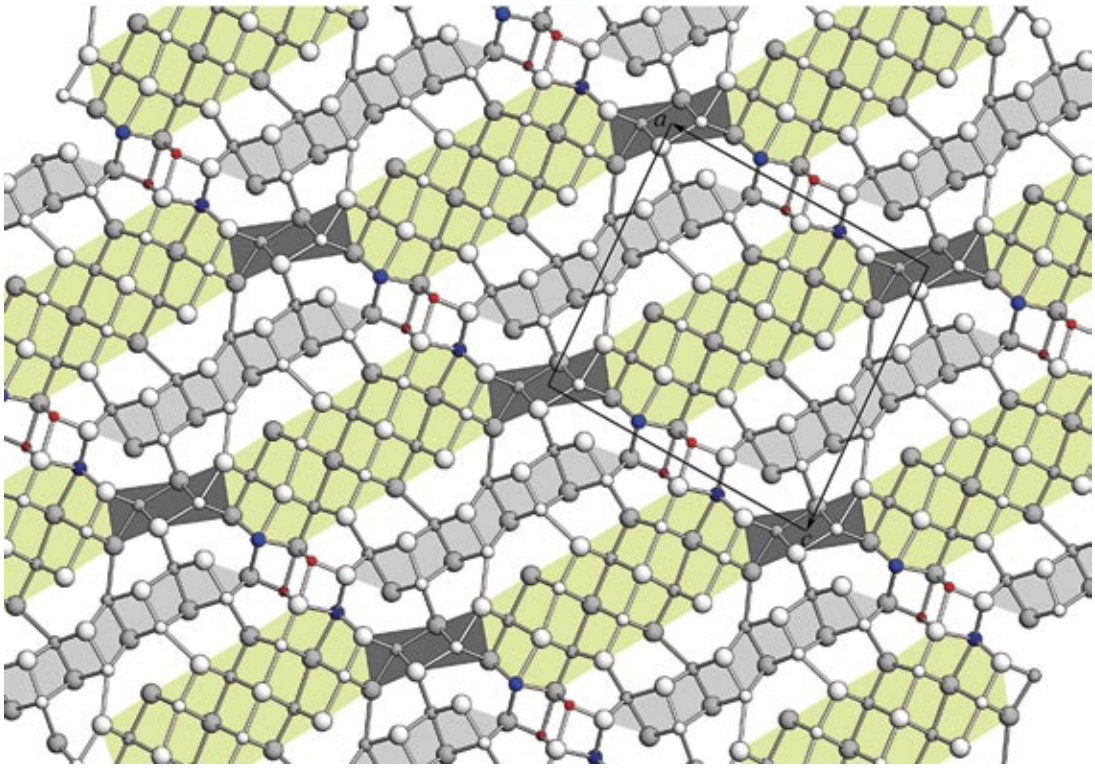

FIG. 7. The crystal structure of nordströmite, $CuPb_3Bi_7(S,Se)_{14}$ (Mumme 1980), a structure related to the hypothetical QQ sequence described in Figure 5. A description is provided in the text.

TABLE 7. UNIT-CELL AND COMPOSITION DATA FOR DERIVATIVES OF PADĚRAITE

No.	Mineral	modules	*a* (Å)	*b* (Å)	*c* (Å)	β (°)	d_{001} (Å)	S.G.	Formulae	Fig.
1	paděraite	P = Q + K	17.6	3.9	28.5	105.4	27.5	$P2_1/m$	$Cu_{14}Me^{2+}{}_4Bi_{22}S_{44}$	3
2	Q str.1	..QQ..	17.6	3.9	16.5	114	15.1	$P2_1/m$	$Cu_6Me^{2+}{}_6Bi_{10}S_{24}$	5
3	Q str.2	..QQ'..	17.6	3.9	31.1	100	30.6	$A2/m$	$Cu_{12}Me^{2+}{}_{12}Bi_{20}S_{48}$	6
4	homologue	KQQ, KQQ'	17.6	3.9	43.2	92	43.2	(1), (2)	$Cu_{20}Me^{2+}{}_{10}Bi_{32}S_{68}$	10a, b
5	intergrowth	P + K	17.6	3.9	40.2	94	40.1	$P2_1/m$	$Cu_{22}Me^{2+}{}_8Bi_{34}S_{64}$	9b
6	intergrowth	P + C	17.6	3.9	44.3	104	43	$P2_1/m$	$Cu_{22}Me^{2+}{}_6Bi_{34}S_{68}$	9a
7	intergrowth	P + H	17.6	3.9	53.6	97	53.3	Pm	$Cu_{30}Me^{2+}{}_4Bi_{46}S_{88}$	9c
8	polytype II	ODL1, 2	17.6	3.9	55	93	54.9	$A2/m$	$Cu_{28}Me^{2+}{}_8Bi_{44}S_{88}$	8

(1) KQQ: $P2_1/m$, (2) KQQ': $P2/m$. A part of the Me^{2+} in the idealized formulae can be replaced by Ag + Bi. A small part of the Bi can be replaced by copper, as in the paděraite structure from Swartberg. A small part of Cu in the idealized formulae #4, #5 and #7 can be replaced by Fe^{3+}, as in the structure of kupčikite.

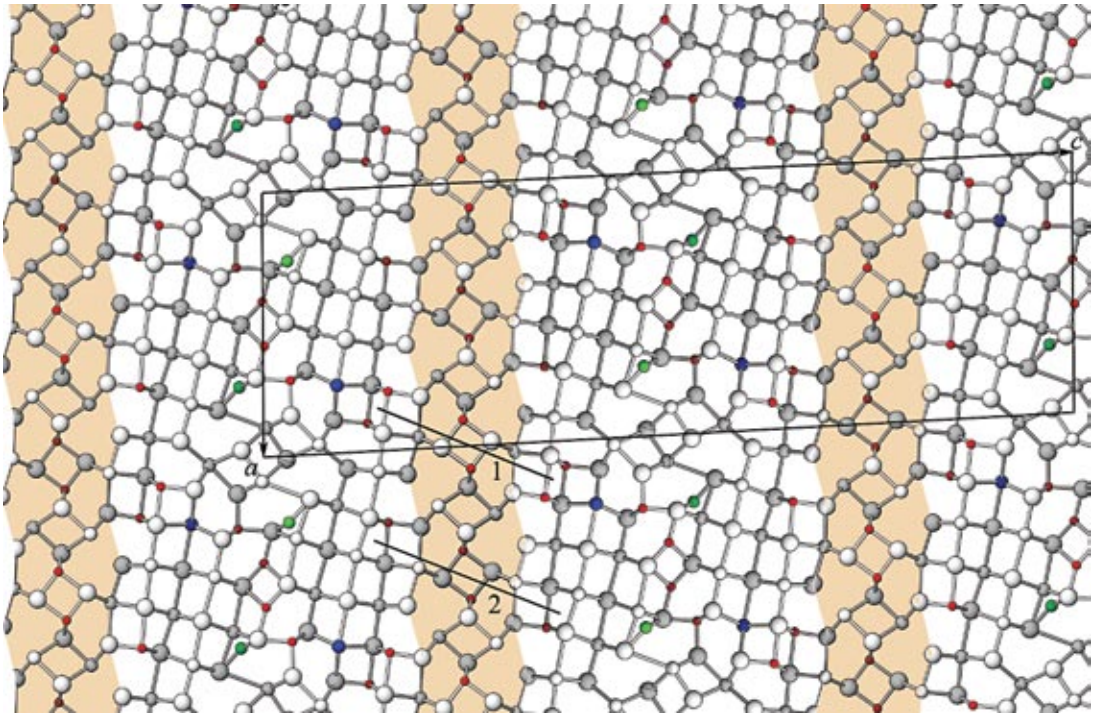

FIG. 8. The alternative, hypothetical polytype of paděraite with the adjacent ODL2 layers displaced by (***a*** + ***b***)/2 across each intervening ODL1 layer. Line segments 1 and 2 interconnecting the copper configurations are used to illustrate the nature of OD phenomena. They should be compared with the line segment 3 in Figure 3.

(1986), has been confirmed by HRTEM observations of Ciobanu *et al.* (2004), who observed parallel intergrowths of paděraite and cuprobismutite. None of the observed sections revealed longer-range superperiodicities; up to two or three repetitions of 1:1, 1:2 and 1:3 combinations of paděraite and cuprobismutite cells were observed intergrown with longer sequences of pure phases separated by mixed transitional zones.

These observations lead us to the models of paděraite–kupčíkite, paděraite–hodrushite, and paděraite–cuprobismutite intergrowths (Fig. 9), limited here to 1:1 ratios because of their large unit-cells. The

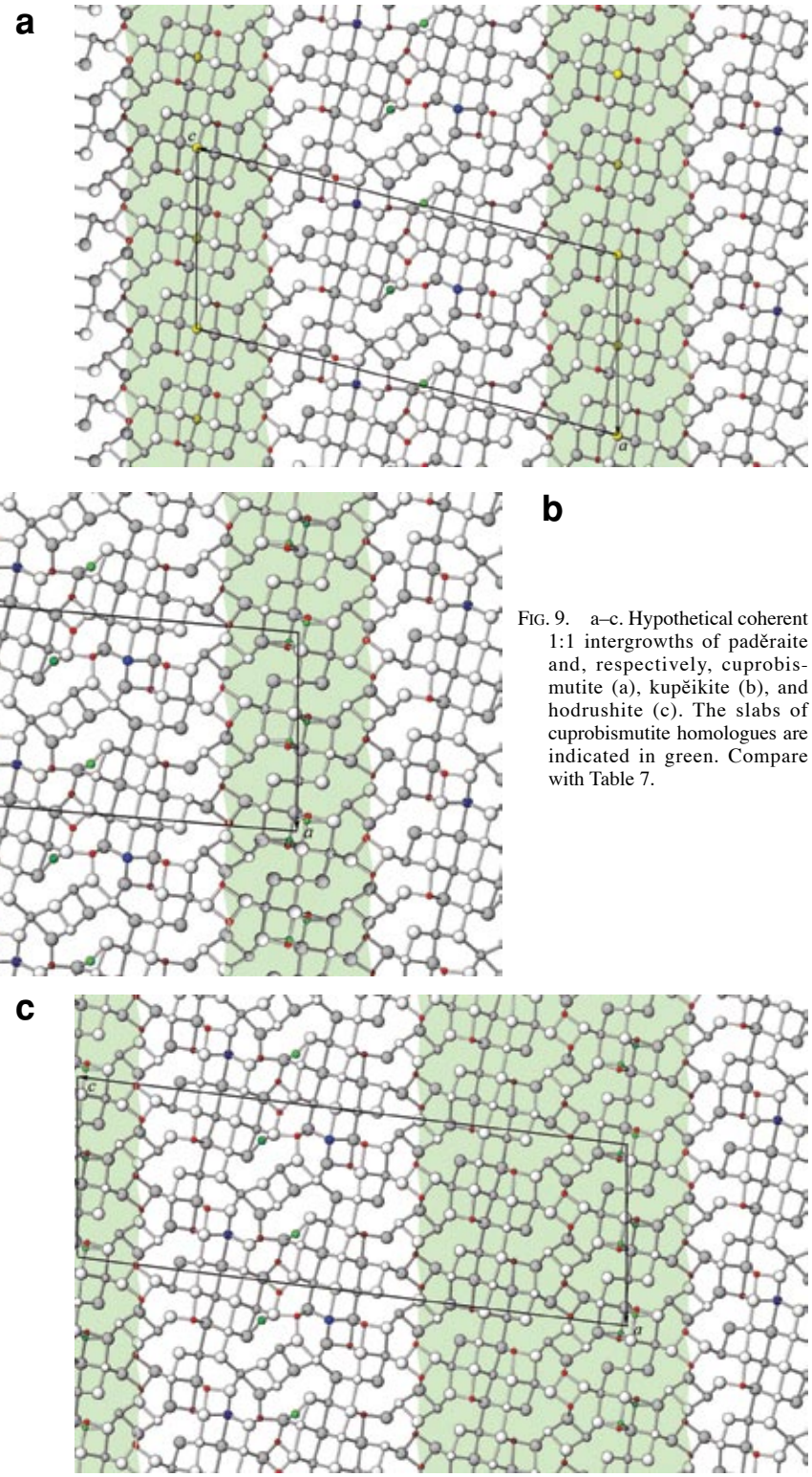

FIG. 9. a–c. Hypothetical coherent 1:1 intergrowths of paděraite and, respectively, cuprobismutite (a), kupčikite (b), and hodrushite (c). The slabs of cuprobismutite homologues are indicated in green. Compare with Table 7.

structure of natural Ag-bearing cuprobismutite, determined by Topa *et al*. (2003b), was used instead of the Cu-rich synthetic version used by Ciobanu *et al*. (2004) in their modeling. Idealized unit-cell data for these intergrowths are presented in Table 7. The general formula of the paděraite:cuprobismutite = 1:N series PC^n is then: $Cu_{14+8N}Me^{2+}{}_{4+2N}Bi_{22+12N}S_{44+24N}$, where N is the number of cuprobismutite-like slabs alternating with one paděraite-like slab. The thickness of these unit slabs is defined in Figures 9a–c. The general formulae for the paděraite:kupčíkite = 1:N series PK^n and paděraite:hodrushite = 1:N series PH^n can be also derived, using data from Table 7.

The decomposition of paděraite into two slabs, a kupčíkite-like one (K in Fig. 3) and the "remaining" one (Q in Fig. 3), leads to a potential homologous series KQ^n : $Cu_{8+6N}Me^{2+}{}_{6N-2}Bi_{12+10N}S_{20+24N}$ exemplified by paděraite itself (a KQ homologue, n = 1) (Fig. 3) and the next higher homologues KQ^2 of both kinds (KQQ and KQQ'), shown in Figures 10a and 10b, respectively (see also Table 7). The opposite trend, K^nQ, is exemplified by the paděraite–kupčíkite intergrowth, which actually is the homologue K^2Q.

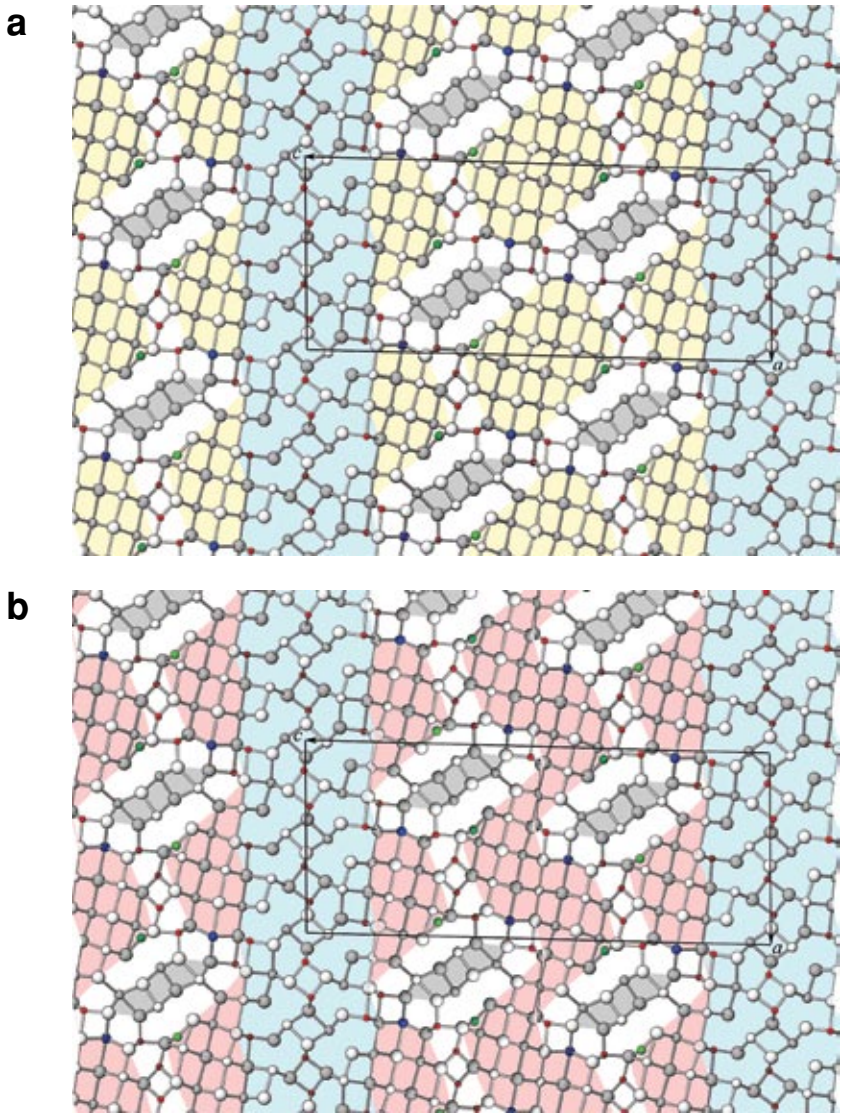

FIG. 10. a, b. The hypothetical kupčikite-Q layer homologues KQQ and KQQ' (compare with Figs. 5 and 6). The kupčikite K modules are colored in blue.

The origin of these intergrowths seems to be complicated. Our observations by reflected light microscopy suggest a replacement of Cu-enriched hodrushite by Cu-enriched paděraite in the material from Swartberg. The Băiţa Bihor material suggests the same trend. As already mentioned, the later replacements by makovickyite and bismuthinite–aikinite derivatives help to obscure the original replacement-intergrowth relationships.

Acknowledgements

The material from Băiţa Bihor was kindly supplied by Prof. W.H. Paar (Salzburg) and Prof. G. Cioflica (Bucharest), whereas that from Swartberg was made available by Prof. R. Merkle (Pretoria) and by Drs. N. Cook and C.L. Ciobanu (Oslo). This study was supported by the Austrian Science Fund (FWF), research project P17349–N10. The assistance of Mrs. Camilla Sarantaris is gratefully acknowledged. The manuscript benefitted from comments of Drs. A. Pring and C.L. Ciobanu, as well as from the comments and editorial care of Prof. Robert F. Martin.

References

Balić-Žunić, T. & Makovicky, E. (1996): Determination of the centroid or 'the best centre' of a coordination polyhedron. *Acta Crystallogr.* **B52**, 78-81.

Balić-Žunić, T. & Vicković, I. (1996): IVTON – a program for the calculation of geometrical aspects of crystal structures and some crystal chemical applications. *J. Appl. Crystallogr.* **29**, 305-306.

Bruker AXS (1998): SMART, V. 5.0. Brucker AXS, Inc., Madison, Wisconsin 53719, USA

Bruker AXS (1997): SHELXTL, V. 5.1. Brucker AXS, Inc., Madison, Wisconsin 53719, USA

Cook, N.J. & Ciobanu, C.L. (2003): Lamellar minerals of the cuprobismutite series and related paděraite: a new occurrence and implications. *Can. Mineral.* **41**, 441-456.

Ciobanu, C.L., Pring, A. & Cook, N.J. (2004): Micron- to nano-scale intergrowths among members of the cuprobismutite series and paděraite: HRTEM and microanalytical evidence. *Mineral. Mag.* **68**, 279-300.

Kupčík, V. & Makovicky, E. (1968): Die Kristallstruktur des Minerals (Pb,Ag,Bi)$Cu_4Bi_5S_{11}$. *Neues Jahrb. Mineral., Monatsh.*, 236-237.

Makovicky, E. (1989): Modular classification of sulfosalts – current status: definition and application of homologous series. *Neues Jahrb. Mineral., Abh.* **160**, 269-297.

Makovicky, E. & Balić-Žunić, T. (1998): New measure of distortion for coordination polyhedra. *Acta Crystallogr.* **B54**, 766-773.

Makovicky, E., Balić-Žunić, T. & Topa, D. (2001): The crystal structure of neyite, $Ag_2Cu_6Pb_{25}Bi_{26}S_{68}$. *Can. Mineral.* **39**, 1365-1376.

Mariolacos, K., Kupčík, V., Ohmasa, M. & Miehe, G. (1975): The crystal structure of $Cu_4Bi_5S_{10}$ and its relation to the structures of hodrushite and cuprobismutite. *Acta Crystallogr.* **B31**, 703-708.

Miehe, G. (1971): Crystal structure of kobellite. *Nature Phys. Sci.* **231**, 133-134.

Mumme, W.G. (1980): The crystal structure of nordströmite $CuPb_3Bi_7(S,Se)_{14}$, from Falun, Sweden: a member of the junoite homologous series. *Can. Mineral.* **18**, 343-352.

Mumme, W.G. (1986): The crystal structure of paděraite, a mineral of the cuprobismutite series. *Can. Mineral.* **24**, 513-521.

Mumme, W.G. & Žák, L. (1985): Paděraite $Cu_{5.9}Ag_{1.3}Pb_{1.6}Bi_{11.6}S_{22}$, a new member of the cuprobismutite–hodrushite group. *Neues Jahrb. Mineral., Monatsh.*, 557-567.

Sheldrick, G.M. (1997a): *Shelxs–97. A Computer Program for Crystal Structure Determination*. University of Göttingen, Göttingen, Germany.

Sheldrick, G.M. (1997b): *Shelxl–97. A Computer Program for Crystal Structure Refinement*. University of Göttingen, Göttingen, Germany.

Topa, D., Makovicky, E. & Balić-Žunić, T. (2003b): Crystal structures and crystal chemistry of the members of the cuprobismutite homologous series of sulfosalts. *Can. Mineral.* **41**, 1481-1501.

Topa, D., Makovicky, E., Balić-Žunić, T. & Paar, W.H. (2003a): Kupčíkite, $Cu_{3.4}Fe_{0.6}Bi_5S_{10}$, a new Cu–Bi-sulfosalt from Felbertal, Austria, and its crystal structure. *Can. Mineral.* **41**, 1155-1166.

Received February 17, 2005, revised manuscript accepted July 15, 2005.